Eolian sand and loess deposits indicate west-northwest paleowinds during the Late Pleistocene in western Wisconsin, USA

Randall J. Schaetzl[a]*, Phillip H. Larson[b], Douglas J. Faulkner[c], Garry L. Running[c], Harry M. Jol[c], Tammy M. Rittenour[d]

[a]Department of Geography, Environment, and Spatial Sciences, Michigan State University, East Lansing, Michigan 48823, USA
[b]Department of Geography, AGES Research Laboratory, Minnesota State University, Mankato, Minnesota 56001, USA
[c]Department of Geography and Anthropology, University of Wisconsin–Eau Claire, Eau Claire, Wisconsin 54701, USA
[d]Department of Geology, Luminescence Laboratory, Utah State University, Logan, Utah 84322, USA

Abstract

Our study adds to the Quaternary history of eolian systems and deposits in western Wisconsin, USA, primarily within the lower Chippewa River valley. Thickness and textural patterns of loess deposits in the region indicate transport by west-northwesterly and westerly winds. Loess is thickest and coarsest on the southeastern flanks of large bedrock ridges and uplands, similar in some ways to shadow dunes. In many areas, sand was transported up and onto the western flanks of bedrock ridges as sand ramps, presumably as loess was deposited in their lee. Long, linear dunes, common on the sandy lowlands of the Chippewa valley, also trend to the east-southeast. Small depressional blowouts are widespread here as well and often lie immediately upwind of small parabolic dunes. Finally, in areas where sediment was being exposed by erosion along cutbanks of the Chippewa River, sand appears to have been transported up and onto the terrace treads, forming cliff-top dunes. Luminescence data indicate that this activity has continued throughout the latest Pleistocene and into the mid-Holocene. Together, these landforms and sediments paint a picture of a locally destabilized landscape with widespread eolian activity throughout much of the postglacial period.

Keywords: Loess; Parabolic dunes; Sand ramps; Linear dunes; Shadow dunes

INTRODUCTION

Our understanding of eolian systems of the past is usually either derived from modeled data or interpreted from ground data (e.g., the orientations and sedimentology of eolian landforms or spatial trends in eolian sediments such as loess or cover sand). The most commonly used small-scale model for such applications is the COHMAP (Cooperative Holocene Mapping Project) model (COHMAP Members, 1988), which depicts a glacial anticyclone near the southern margins of the Laurentide Ice Sheet (LIS) in summer (Hobbs, 1943; Bryson and Wendland, 1967). Data from large spits, eroded headlands on islands, and deltas in glacial Lake Algonquin, which spanned the southern margins of the ice sheet in the upper Great Lakes region between 13,300 and 11,500 cal yr BP, point to strong easterly winds within ≈150–200 km of the ice front (Krist and Schaetzl, 2001; Vader et al., 2012; Schaetzl et al., 2016). Such winds, at a latitude normally

dominated by westerly flow, support the concept of a glacial anticyclone, as do dune orientations in Saskatchewan, Canada (David, 1981), and other on-ground data (for a review, see Schaetzl et al., 2016). Thus, ground data, if they derive from wind-influenced deposits or landforms at or near former ice marginal locations, can often be used to test the veracity of modeled data.

Nonetheless, the spits and islands of glacial Lake Algonquin are all immediately proximal to a part of the ice sheet with a generally east-to-west trending margin, where easterly winds would have been minimally disrupted by the geography of the ice margin. Other locations, where more lobate ice sheet margins existed, would undoubtedly have had much more complex wind patterns. Our study area is one such example. Another is in northeastern Wisconsin, where, based on textural and thickness patterns of loess, Schaetzl and Attig (2013) reported evidence for easterly and westerly winds, presumably influenced by katabatic winds off the Lake Michigan and Ontonogan/Keweenaw Bay lobes. Small deposits of loess in Michigan's Upper Peninsula also point to loess deposits formed on variable winds, perhaps resulting from the complex interaction of katabatic winds with the

---

*Corresponding author at: Department of Geography, Environment, and Spatial Sciences, Michigan State University, East Lansing, Michigan 48823, USA. E-mail address: soils@msu.edu (R.J. Schaetzl).

westerlies, coupled with a weakening glacial anticyclone (Kilibardia and Blockland, 2011; Luehmann et al., 2013). Thus, additional ground data from other eolian features and deposits in the Great Lakes region could help refine our understanding of paleocirculation patterns and atmospheric drivers of eolian deposition in this region at the last glacial maximum (LGM) and continuing into the Holocene.

Slowly, data continue to accrue on the strength, directionality, and geographic extent of past eolian systems in the Great Lakes region. For example, research on sand dune orientations in the central Great Lakes region, for the period 14,000 to 10,000 yr BP, provides data for westerly winds at locations not near the ice margin during the latest Pleistocene. Dunes in central Lower Michigan—only about 200–250 km south of the ice margin—suggest that westerly and northwesterly winds were dominant here between 13,000 and 10,000 yr BP (Arbogast et al., 2015; Fig. 1). Dunes in central
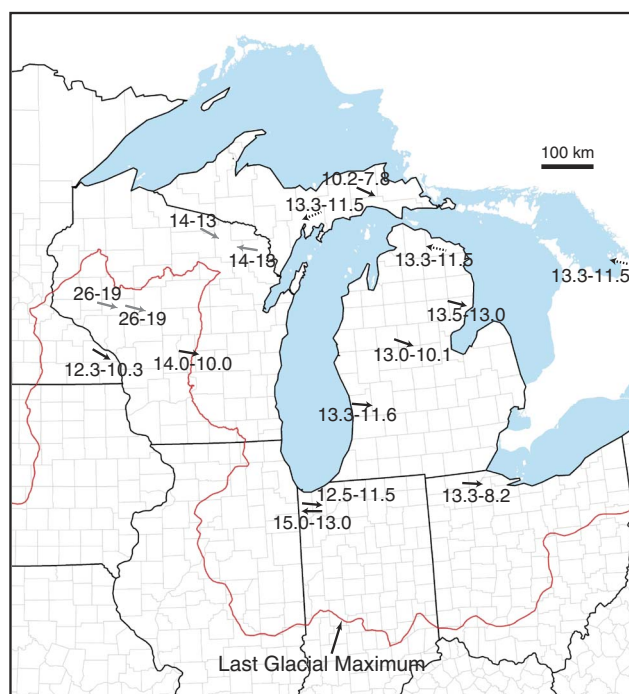

Figure 1. (color online) Locations of study sites in the upper Midwest that report on wind directions in the Late Pleistocene or early Holocene. Dune sites near the Great Lakes' shoreline are not shown because they are influenced by not only regional winds but also local winds and sand supply, and because they cannot build out, into the lake, even if prevailing winds would force that to happen. Large-scale, Late Pleistocene transport of loess on generally westerly winds, out of north–south flowing meltwater river valleys, has long been known for this region and is therefore not shown here. Compiled from Arbogast et al. (2015, 2017), Campbell et al. (2011), Colgan et al. (2017), Hanson et al. (2015), Kilibarda and Blockland (2011), Krist and Schaetzl (2001), Loope et al. (2004), Rawling et al. (2008), Schaetzl et al. (2014, 2016), Stanley and Schaetzl (2011), and Vader et al. (2012). Black arrows indicate data from dunes, gray arrows indicate data from loess, dashed arrows indicate data from spits or other features. Ages shown are best estimates based on ages cited in the original paper or the best estimates of the authors.

Wisconsin, slightly farther from the ice margin, were also formed by westerly winds between 14,000 and 10,000 yr BP (Rawling et al., 2008). In the Driftless Area of Minnesota near the Root River, eolian sands were deposited as sand ramps and on ridge crests on slopes facing north-northwest, indicating transport by northwesterly winds. Basal sands here were deposited between 12,300 and 10,300 yr BP (Hanson et al., 2015). Elsewhere in Minnesota, predominantly northwesterly winds drove Holocene eolian systems (Grigal et al., 1976; Keen and Shane, 1990).

Despite our growing understanding of Quaternary eolian systems in this region, a considerable number of spatial and temporal gaps remain (Fig. 1). Ground data from underrepresented areas and for systems of different (or unknown) ages are key to refining any models or resolving any hypotheses about past eolian systems in this region. Such data are also needed to help interpret their spatiotemporal linkages to other geomorphic systems and to evaluate their paleoenvironmental significance. Our work is designed to address this gap by focusing on eolian systems and landforms in western and west-central Wisconsin, to help understand eolian systems here during the Late Pleistocene and into the Holocene, focusing on the lower Chippewa River valley (LCRV). Not only do deposits and landforms here suggest a strong west-northwesterly wind regime during the immediate postglacial period, but the widespread nature and longevity of eolian activity here points to a landscape that was unstable for considerable periods of time.

We argue that ground data on eolian sediments and landforms can assist paleoclimate models and help us to understand the postglacial climate of the region. Because the study area contains many bedrock ridges and inselbergs, we hypothesize that the pattern of eolian sediments and features near such "obstructions" may provide insight into paleowind directionality and strength. To that end, we will describe a variety of sandy and silty eolian deposits and landforms in the LCRV, to estimate the direction of winds responsible for their formation. Age data, limited though it may be at present, will help establish a preliminary chronology for some of these deposits.

STUDY AREA

Much of our work is focused in or near the LCRV, immediately south on the terminal moraine of the LIS (Fig. 2; Faulkner et al., 2016). The Chippewa River is a major tributary to the upper Mississippi River in west-central Wisconsin. The upper Chippewa watershed was glaciated during Marine Oxygen Isotope Stage (MIS) 2 (i.e., the Late Wisconsinan glaciation). MIS 2 ice advanced into the Chippewa River basin from the north, as part of the Chippewa lobe, between ca. 18,500 and 22,000 yr ago (Schaetzl et al., 2014). Nonetheless, chronological control on the maximal ice advance, and on the initiation of ice retreat, is not well constrained (Mickelson et al., 1983; Attig et al., 1985; Syverson, 2007). Although the degree of synchronicity of ice marginal retreat in the upper Midwest is uncertain, recent data from Carson et al. (2012) reported that, for a site ≈150 km south of the
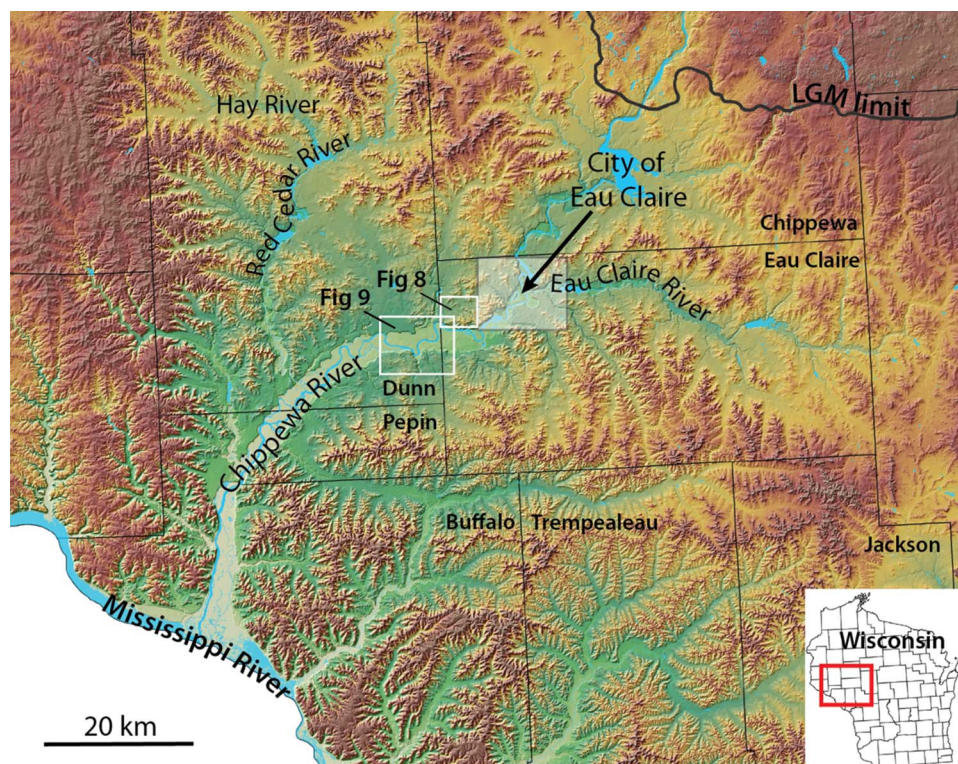
Figure 2. (color online) Topographic representation of the study area of the lower Chippewa River valley, showing the major rivers and counties, the southern limit of Marine Oxygen Isotope Stage 2 glaciation, the extent of Figures 8 and 9, and the general location of the city of Eau Claire. LIDAR (light detection and ranging) data resolutions are 1.52 m (5 ft.) for Chippewa, Eau Claire, and Pepin Counties; 4.57 m (15 ft.) for Dunn County; and 1.0 m (3.28 ft.) for the city of Eau Claire. Elevations on this map range from 199 m (Mississippi River) to 425 m (northern Jackson County). LGM, last glacial maximum.

study area, the Green Bay Lobe was at its maximum position from about 26.4 to 21.4 ka. Earlier, Attig et al. (2011b) had reported that the southern Green Bay Lobe had begun to recede by about 18.5 ka. During the LGM and for a considerable time afterward, continuous permafrost likely extended from at least 20 km to perhaps as far as 90 km beyond the ice margin (Johnson, 1986; Ham and Attig, 1997; Clayton et al., 2001; Mason, 2015).

Much of the study area south of the LGM ice margin was glaciated before MIS 2, although the exact ages of the glacial deposits are still being debated (Baker et al., 1983; Syverson and Colgan, 2004; Attig et al., 2011a; Schaetzl et al., 2014). Here, glacial deposits can be found only in protected landscape positions and are largely absent in the southwestern parts of the region. Finally, the farthest southwestern and southern parts of the area display little evidence for past glaciation and, hence, are probably part of Wisconsin's Driftless Area (Knox et al., 1982).

South of the terminal moraine, where glacial deposits are thin or nonexistent, the landscape is dominated by dissected bedrock uplands. Valleys are variously filled with glacial outwash, sandy colluvium, or combinations of both. The bedrock is composed of weak, fine-grained sandstones (Ostrom, 1970; Brown, 1988) in the north, leading to rounded inselbergs and generally gentle, pediment-like slopes. Nearer the Mississippi valley, uplands are often flatter

because of a cap of carbonate rocks, primarily dolomites (Brown, 1988).

During the Late Wisconsinan, the Chippewa River was a major meltwater stream, as were its largest tributaries, the Eau Claire, Hay, and Red Cedar Rivers (Fig. 2). Typical of glacial meltwater streams in general, the Chippewa and its main tributaries aggraded their valleys with thick deposits of outwash. Then, with the onset of regional deglaciation, they began incising into their glaciofluvial fills, forming conspicuous suites of inset terraces (Faulkner et al., 2016). Existing evidence indicates that terrace cutting was initiated by base-level fall driven by at least two episodes of Mississippi River incision prior to 13.4 ka. Subsequently, incision progressed up the Chippewa valley in a prolonged, episodic manner, leaving behind a meltwater braidplain as a prominent high terrace—the Wissota Terrace (Andrews, 1965), which can be traced up the valleys of the Chippewa River's incised tributary streams (Faulkner et al., 2016).

Above the bedrock, residuum, and glaciofluvial deposits that aggraded in valleys, the landscape is variously mantled with a thin cover of eolian deposits, many of which are sandy (Weidman, 1911). Ventifacts on some of the older (pre–MIS 2) surfaces attest to the intensity of paleowinds here, at some time in the past (Syverson, 2007). Soils on the sandstone uplands are largely formed in sandstone residuum—typically sandy loam in the upper profile, grading

to fine sandy loam textures at depth. Nonetheless, official descriptions of several soil series from local soil surveys also explicitly mention eolian sands as parent materials. In other county soil surveys, such sediments can be inferred based on textural characteristics (i.e., textures ranging from fine sand to fine-to-medium loamy sand). Eolian sands here are often subtle, thin, and widely scattered; there are no major dune fields. Indeed, it is often difficult to distinguish eolian sand from residuum or outwash. An important identifying feature used in the LCRV is the mixed mineralogy of the outwash sands, which were derived from a wide variety of crystalline rocks to the north. Sands derived from bedrock residuum tend to be much more quartz rich and a distinctly different ("whiter") color.

Possible sources for eolian sands in the LCRV include (1) sandstone residuum on uplands; (2) sandy glaciofluvial deposits in the valley proper; (3) gravelly sandy loam, pre–MIS 2 tills; and (4) gravelly sand alluvium, also pre–MIS 2 in age (Syverson, 2007). Although the widespread occurrence of sandy eolian deposits in the LCRV has been recognized for more than a century (Weidman, 1911), they have not been thoroughly investigated and remain poorly understood. Almost no data exist regarding their depositional chronology, paleoenvironmental significance, or origin.

Because most of this landscape is sloping and hence subject to erosion, loess deposits vary greatly in thickness. Many of the loess deposits are spatially disjunct, and many areas lack loess entirely (Schaetzl et al., 2014; Fig. 3).

Where thin, loess deposits are loamy, because they have been intermixed with the underlying residuum. Loess is especially thick on uplands near the Mississippi River (Hole, 1976; Scull and Schaetzl, 2011). Much of this loess was likely derived from the valley while it functioned as a major meltwater sluiceway (Leigh and Knox, 1993; Bettis et al., 2003; Schaetzl et al., 2014) and from sources farther west. Locally, especially east of the Chippewa River, loess deposits appear to be linked, at least in part, to the Chippewa River valley train (Schaetzl et al., 2014). Loess deposits farther east are thinner and quite spatially discontinuous (Scull and Schaetzl, 2011; Stanley and Schaetzl, 2011; Fig. 3). Nonetheless, in preferred sites on stable uplands, loess thicknesses can exceed 3 m, even as nearby landscapes have no detectable loess (Schaetzl et al., 2014). Often, areas with thin or undetectable amounts of loess occur on sandy side slopes and in lowlands, which may have been unstable during the postglacial permafrost period, and/or which may have acted as a transportation surface for silts (Stanley and Schaetzl, 2011). In the latter situation, saltating sands impact loess deposits that are accruing, remobilizing them and facilitating their continued transport downwind (Mason et al., 1999; Syverson, 2007). This process continues until a barrier to sand transport is encountered (e.g., a deep river valley, a steep escarpment, or an abrupt upland). Loess then accumulates downwind of the topographic obstruction in the transportation surface.
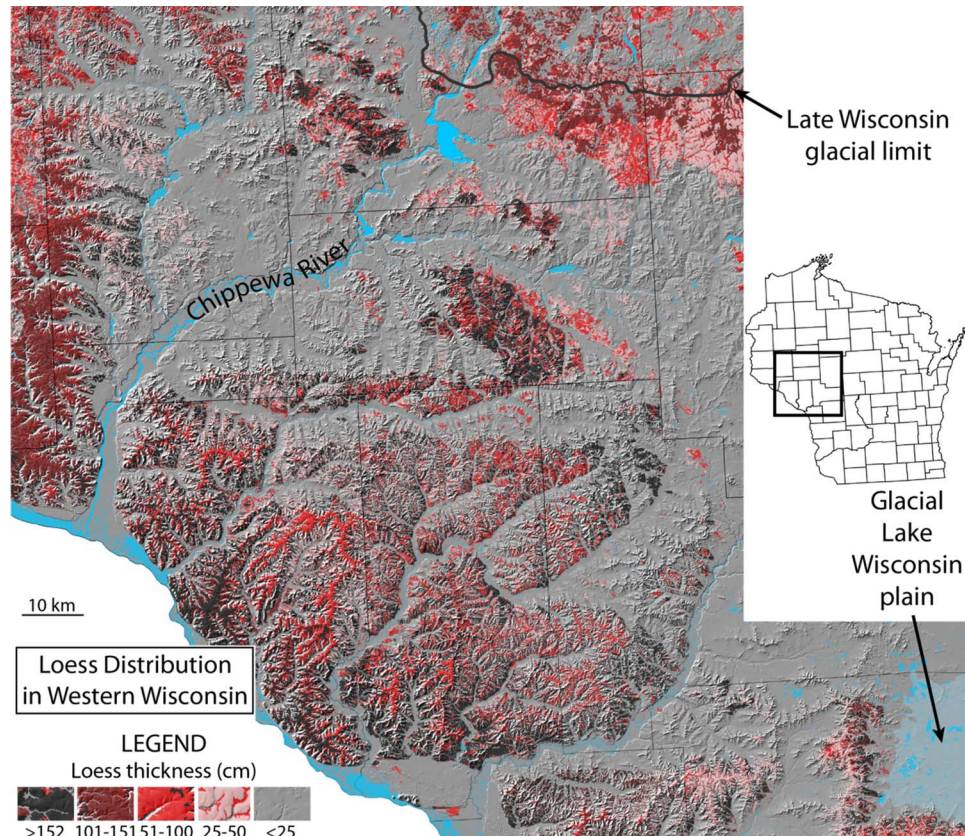

Figure 3. (color online) Extent and thickness of loess within the study area, as derived from Natural Resources Conservation Service county soil surveys.

METHODS

Loess mapping and sampling

As has been done previously (Stanley and Schaetzl, 2011; Luehmann et al., 2013; Schaetzl and Attig, 2013), county soil survey data for the study area were downloaded from the Natural Resources Conservation Service, imported into geographic information system (GIS) and rasterized. For soils developed in loess, as described in their official series descriptions (OSDs), we determined the typical loess thickness from the OSDs, entered the value into a GIS attribute table, and used these data to code the GIS map unit symbology. Texture data for the uppermost and deepest mineral horizons were also coded into the GIS. The GIS data were then loaded onto a laptop computer, equipped with GPS, to facilitate field navigation to predetermined, potential sampling sites. Our field sampling goal was to obtain loess samples from numerous broad, stable uplands. Loess was sampled with a hand auger at 223 sites on stable uplands. All samples were obtained within or below the soil profile, but at least ≈30 cm from any underlying sediment or bedrock. We sampled so as to obtain an amalgamated representation of the entire loess column.

We also used a GIS, in conjunction with NRCS county-level soils data, to evaluate the distribution and thickness of loess deposits near major bedrock inselbergs, ridges, and uplands (Fig. 4). Such data were used to test the hypothesis that loess is preferentially deposited on, primarily, one side of large ridges and isolated uplands. This hypothesis suggests these prominent topographic barriers act as a wind obstruction and, thus, facilitate loess deposition in their lee. Loess should, theoretically, accumulate preferentially on one side of the ridge if the paleowinds that transported the loess originated mainly from one direction (Hesp and Smyth, 2017). Similar features, on smaller scales, occur in eolian sand systems, where they are referred to as nebkha or shadow dunes (Hesp, 1981). For each of 104 sites, we estimated loess thickness at distances of 0.5, 1.0, 1.5, and 2.0 km from the ridgetop, along eight cardinal directions, in a GIS (Fig. 4B). Loess thickness were categorized from NRCS county soil data, with ordinal thickness categories as follows: > 60 inches (5), 40–60 inches (4), 20–40 inches (3), 10–20 inches (1), and sites where loess soils are not mapped (0).

Loess and loess data analyses

Loess samples were air-dried, lightly ground to pass a 2 mm sieve, and passed through a sample splitter three times, in order to achieve the homogeneity necessary for laser particle-size diffraction on a Malvern Mastersizer. From each sample, a 2 g subsample was dispersed in a water-based solution of $(NaPO_3)_{13} \cdot Na_2O$, after shaking for 30 min. As discussed in Miller and Schaetzl (2012), small subsamples analyzed in laser particle-size analyzers are not always representative. Thus, we analyzed two subsamples from each loess sample and compared the data. In cases where the suite of particle-size data were sufficiently similar statistically, we used the mean values for all subsequent analyses. However, in cases where the data from the two runs were sufficiently dissimilar (for details, see Miller and Schaetzl, 2012), a third, or sometimes fourth, subsample was run, and the two most comparable samples were used to generate the mean values used in subsequent analyses.

Loess deposits are often mixed with underlying sediment, especially in areas known to have had permafrost (McSweeney et al., 1988; Luehmann et al., 2013; Schaetzl and Attig, 2013; Schaetzl and Luehmann, 2013). In our study area, mixing of loess with sandstone residuum below is common, as evidenced by bimodality in the particle-size curves. Therefore, we followed the practice of Luehmann et al. (2013), and "filtered" the particle-size data (i.e., adjusting the particle sizes by removing the sediment that comprises the coarser "peak" and recalculating the remaining textural data). The goal of the filtering process is to restore the particle-size data as close as possible to the presumed original composition. Because most of our loess samples were from thick deposits, they lacked a second (sand) peak, and the filtering process left the original particle-size data unchanged. Nonetheless, for sites shallow to sandstone residuum, the filtering process performs an important function—restoring the particle-size data of the loess to a condition closer to its original state.

Sandy eolian deposits and landforms

Fieldwork in the study area, associated with several previous studies (Larson et al., 2008; Olson et al., 2008; Faulkner et al., 2016), identified potential sandy eolian deposits and landforms. Particularly, Larson et al. (2008) investigated a landform that, based on morphology, internal sedimentary structures, textural analysis, and landscape position adjacent to the Wissota Terrace scarp, was interpreted as a cliff-top parabolic dune. Their work was, however, restricted to this single location (Fig. 2). Olson et al. (2008) then attempted to identify and map sandy eolian deposits across the region, using NRCS county soils data, concluding that sandy eolian deposits are widespread throughout the LCRV, but the resolution of their predictive mapping left uncertainty regarding the exact distribution and morphology of a variety of such landforms. The studies by both Larson et al. (2008) and Olson et al. (2008) were preliminary investigations, limited in scope, and conducted without the aid of high-resolution light detection and ranging (LIDAR)–derived digital elevation models (DEMs). In the present study, we undertook a more detailed inventory of sandy eolian landforms, based on sand textures (from soil survey data) of landforms with dune-shaped morphologies and by utilizing recently acquired LIDAR data that range in resolution from 0.9 m (3 ft.) to 4.6 m (15 ft.) cell sizes. Dune morphologies were then used to interpret former wind directions. We derived a preliminary chronology of these landforms, based on stratigraphic relationships with other deposits of known age, as well as absolute age control on some archetypical landforms.
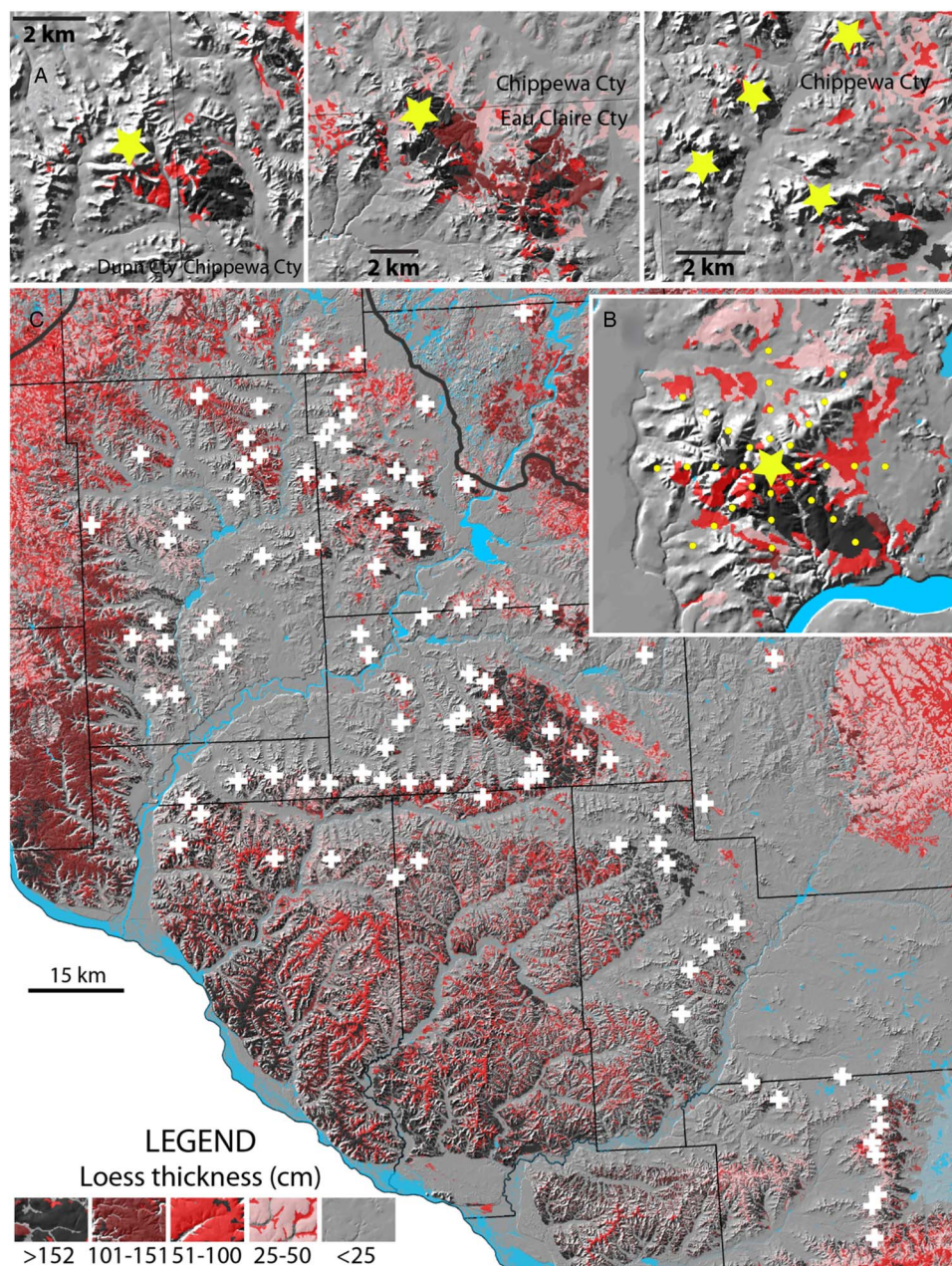
Figure 4. Loess distribution across the study area, showing the locations of sample sites (white crosses) near bedrock uplands. (A) Three representative sites, characteristic of loess distribution near isolated bedrock uplands. Note the much thicker loess on the eastern and southeastern flanks of all of these upland areas. The yellow stars represent the midpoints of the sample grids, as shown in panel B. (B) Another such site, showing the distribution of loess and of sample points used in the geographic information system to estimate loess thickness along eight cardinal directions, at 0.5, 1.0, 1.5, and 2.0 km from the center of the ridge (yellow star). (C) The full distribution of the 104 sample points used to estimate patterns of loess thickness and distribution near isolated bedrock uplands. (For interpretation of the references to color in this figure legend, the reader is referred to the web version of this article.)

Luminescence dating

Nine samples were collected from the Roy Street Dune (RSD) for luminescence dating, investigated initially by Larson et al. (2008). At the RSD, four samples were collected using a Geoprobe hydraulic coring unit, two from 2.93 to 3.05 m depth and 4.09 to 4.21 m depth at the dune crest, and two at 3.1–3.22 m and 4.16–4.28 m depths from the toe slope. The toe slope samples were collected from the underlying Wissota Terrace fill, to frame the depositional age of the dune within the Chippewa River incision model of Faulkner et al. (2016). Finally, five additional samples were collected at ≈1.6 m depth from a series of hand-dug pits, one each on the crest, shoulder, back slope, foot slope, and toe slope of the dune; we viewed these depths as sufficient to avoid bioturbation issues (Hanson et al., 2015).
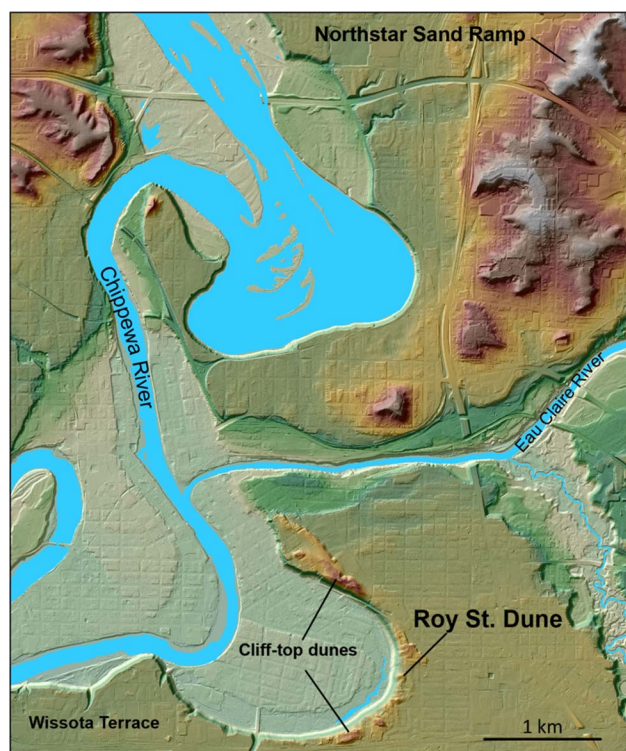
Figure 5. (color online) Map of the area near the Northstar Sand Ramp and Roy Street Dune, near the Chippewa River in the city of Eau Claire. Other dunes, also in cliff-top position, atop the Wissota Terrace, are shown. Elevations on this map range from 241 m (Chippewa River) to 334 m.

Three samples were also recovered using the Geoprobe from the Northstar Sand Ramp (NSR), using a single core, in the middle of the NSR, at depths of 1.79–1.91, 2.73–2.85, and 3.85–3.93 m. Both the RSD and the NSR are located in the city of Eau Claire (Figs. 2 and 5).

Sample processing and optically stimulated luminescence (OSL) analyses were conducted at the Utah State University Luminescence Laboratory. Samples were processed to purify the quartz fine sand fraction (150–250 μm) and followed standard procedures involving wet sieving, gravity separation using sodium polytungstate (2.72 g/cm^3), and acid treatments with HCl and HF to isolate the quartz component. Samples were analyzed following the latest single-aliquot regenerative-dose procedures (Murray and Wintle, 2000, 2003; Wintle and Murray, 2006), and ages were calculated using the central age model of Galbraith and Roberts (2012). Data quality criteria included rejection of aliquots with repeat point signals outside of unity (> ±10%), signal response in the zero-dose step (>10% of natural signal), and feldspar contamination as indicated by response to infrared stimulation (for similar criteria, see Rittenour et al., 2007). Data from rejected aliquots were not included in equivalent dose, overdispersion, or age calculations. OSL ages are reported at 2σ standard error (Table 1).

Dose-rate calculations were determined by chemical analysis of the U, Th, K, and Rb contents using inductively coupled plasma mass spectrometry and inductively coupled plasma atomic emission spectroscopy techniques and conversion factors from Guerin et al. (2011). The contribution of cosmic radiation to the dose rate was calculated using sample depth, elevation, and latitude/longitude following Prescott and Hutton (1994). Dose rates are calculated based on water content, sediment chemistry, and cosmic contribution (Aitken, 1998).

Ground-penetrating radar

We used ground-penetrating radar (GPR) to examine the internal stratigraphy of the RSD, the NSR, and sand sheets ("reflection facies 1" in Faulkner et al. [2016]). GPR is a

Table 1. Luminescence data for the Roy Street Dune (RSD) and Northstar Sand Ramp (NSR) sites.

Sample name	Sample no.	Sample depth (cm)	No. aliquots[a]	Dose rate (Gy/ka)	$D_E \pm 2\sigma$ (Gy)[b]	OD (%)[c]	Age ± 2σ (ka)
RSD-2014-1-Crest	USU-1721	161	20 (40)	1.37 ± 0.07	8.12 ± 1.11	26.3 ± 5.4	5.92 ± 1.01
RSD-2014-2-Shldr	USU-1722	161	11 (30)	1.39 ± 0.08	9.36 ± 0.80	0.0	6.72 ± 0.89
RSD-2014-3-lwr Shldr	USU-1723	160	18 (50)	1.43 ± 0.08	8.73 ± 1.25	22.7 ± 6.3	6.11 ± 1.07
RSD-2014-4-lwr2 Shldr	USU-1724	161	20 (45)	1.35 ± 0.07	8.14 ± 0.89	17.6 ± 4.9	6.03 ± 0.90
RSD-2014-5-lwst Shldr	USU-1725	161	27 (40)	1.33 ± 0.07	8.27 ± 0.64	9.4 ± 4.9	6.21 ± 0.79
RSDshldr (Wissota Terrace)	USU-1880	310–322	16 (43)	1.06 ± 0.06	12.71 ± 1.87	23.9 ± 6.5	12.04 ± 2.15
RSDshldr (Wissota Terrace)	USU-1881	416–428	23 (40)	1.91 ± 0.10	32.46 ± 3.02	16.7 ± 4.2	17.00 ± 2.33
RSDCrest	USU-1882	293–305	19 (43)	1.38 ± 0.07	7.97 ± 1.01	18.1 ± 6.2	5.79 ± 0.94
RSDCrest	USU-1883	409–421	17 (31)	1.33 ± 0.07	8.50 ± 1.11	19.8 ± 6.0	6.37 ± 1.05
NSR-2	USU-1886	179–191	17 (31)	1.66 ± 0.09	16.82 ± 1.55	10.2 ± 5.5	10.12 ± 1.40
NSR-4	USU-1887	385–393	19 (33)	1.61 ± 0.08	17.50 ± 2.00	21.0 ± 4.7	10.85 ± 1.66
NSR-3	USU-1889	273–285	18 (25)	1.74 ± 0.10	18.52 ± 2.03	17.8 ± 4.9	10.67 ± 1.61

[a]Age analysis using the single-aliquot regenerative-dose procedure of Murray and Wintle (2000) on 2 mm small aliquots of quartz sand. Number of aliquots used in age calculation, with number of aliquots analyzed in parentheses.
[b]Equivalent dose (D_E) calculated using the central age model of Galbraith and Roberts (2012).
[c]Overdispersion (OD) represents variance of D_E data beyond the measurement uncertainties. OD values >20% may indicate significant scatter due to depositional or postdepositional processes.

noninvasive, shallow geophysical method in which electromagnetic waves are transmitted into the ground and reflected back to the surface from sedimentary boundaries that have contrasting dielectric properties. GPR has been shown to be particularly well suited to sandy eolian deposits (Havholm et al., 2003, Jol et al., 2003; Baker and Jol, 2007; Bristow, 2009). The details of GPR data collection and interpretation methodologies follow those of Jol and Bristow (2003).

The GPR systems used for the study were Sensors and Software pulseEKKO 100 and 1000 with 200 and 225 MHz antennae, respectively. Step size was 0.1 m, with an antennae separation of 0.5 m. Common midpoint surveys collected in the field were analyzed to determine near-surface velocity, which was used to estimate depth of penetration. Topography along the GPR lines was collected using a laser level to geometrically adjust the resulting transect. The profiles were processed using pusleEKKO software, and we applied an automatic gain control, a dewow filter, and trace-to-trace and down-trace averaging to the wiggle trace plot.

RESULTS AND DISCUSSION

Loess patterns and paleowinds

Previous work has concluded that loess in the LCRV was transported mainly by westerly winds from the valley train systems of the Chippewa and Mississippi Rivers (Schaetzl et al., 2014). The interval for depiction of this loess spans the Late Pleistocene, perhaps peaking between 18 and 13 ka, but likely continuing into the early Holocene (Schaetzl et al., 2014). The widespread presence of thick, relatively coarse loess on uplands east and south of these two large rivers was given as the main reason for these conclusions. Nonetheless, loess is also often quite thick near isolated bedrock uplands, thinning quickly with distance to the east and southeast. Thus, we speculated that the pattern of loess deposition near such features may provide a more detailed understanding of paleowind directions than would a study of the broader, more "regional" loess patterns. Many of the inselbergs stand isolated within a rolling landscape of sandy sediment, often a mix of residuum, colluvium, alluvium, and eolian sands.

Loess is typically thickest on the east-southeastern sides of the large bedrock inselbergs and ridges in the study area (Figs. 3, 4, and 6). Only in the southern part of the study area, by the uplands immediately west of the glacial Lake Wisconsin plain, is loess usually thickest only on the eastern sides of uplands (Fig. 6). The thickest loess is typically encountered at ≈0.5–1.5 km from the inselberg. Loess deposits on the east-southeastern margins of these inselbergs often exceed 2–3 m in thickness and have likely accumulated over millennia during the Late Pleistocene and early Holocene (Schaetzl et al., 2014). Loess is often not even mapped in areas that are west, northwest, north, or northeast of such inselbergs, and >1 km distant (Figs. 4A and B). Frequently, soil textures on the west-northwestern flanks of these same uplands are sandy in texture, suggesting that loess was unable to be retained here, perhaps because they were

transportation and/or erosion surfaces. Such surfaces may in some instances represent sand ramps—eolian sand that is intermittently being transported up and onto the upland, but usually not over it.

In order to better understand the transportation dynamics of loess near bedrock obstructions, we examined "filtered" textural data for 102 sites that are in the immediate lee (mainly southeast) of such obstructions and compared these data to data for loess from 2224 sites throughout Wisconsin and Michigan's Upper Peninsula (Schaetzl and Loope 2008, Scull and Schaetzl 2011, Stanley and Schaetzl 2011, Schaetzl 2012, Luehmann et al. 2013, Schaetzl and Attig 2013, Schaetzl et al. 2014). These data are from loess that spans a variety of depositional settings (Fig. 7). Loess in the lee of uplands in the study area is comparatively depleted in fine silts and sands, and enriched in medium silts, coarse silts, and the finer sand fractions. This partitioning appears to suggest that finer silts are carried far downwind, whereas all but the finest sand fractions are unable to be transported over the upland. Medium and coarse silts are preferentially deposited in the immediate lee of the ridge. In effect, the uplands act as a "snow fence" for loess, much like isolated plants or patches of vegetation act to force deposition of eolian sand in their lees. The clear orientation of these deposits strongly suggests transport of loess on west and northwest winds.

Sand sheets, eolian-dammed drainages, and deflation hollows

Sand sheets are eolian sand deposits characterized by relatively flat or tabular morphologies (Koster, 1988; Kasse, 1997; Ritter et al., 2002; Lancaster, 2009). In cold-climate dune fields, the term sand sheet is used for eolian sand deposits devoid of "dune relief" or slip-face morphologies (Koster, 1988). Sand sheets also tend to drape preexisting topography, resulting in the alternative descriptive term "cover sands" (Kasse, 1997).

While establishing an incision chronology of the alluvial deposits of the LCRV, Faulkner et al. (2016) identified a thin (<1.5 m thick) depositional unit of gravel-free sand overlying the highest terraces, including the highest and oldest Wissota Terrace. This deposit, which they referred to as reflection facies 1 based on GPR data, is common both in exposures and GPR imagery. We interpret this sediment, and other texturally and morphologically similar deposits observed throughout the study area, as sand sheets, although in some locations reflection facies 1 may be paleo-overbank deposits.

In the LCRV, sand sheets are discontinuous, but ubiquitous, commonly found on flat to gently sloping outwash plains and treads of the higher fluvial terraces. Visually, they are difficult to interpret. However, textural analysis suggests that they are distinctly different deposits than the glacio-fluvial sands and Holocene-aged stream terraces they overlie (Faulkner et al., 2016). Sand sheet textures in the LCRV are typically fine sand, loamy fine sand, and loamy sand. More than a dozen soil series descriptions, based on textural characteristics and landscape position, in the Chippewa, Dunn,
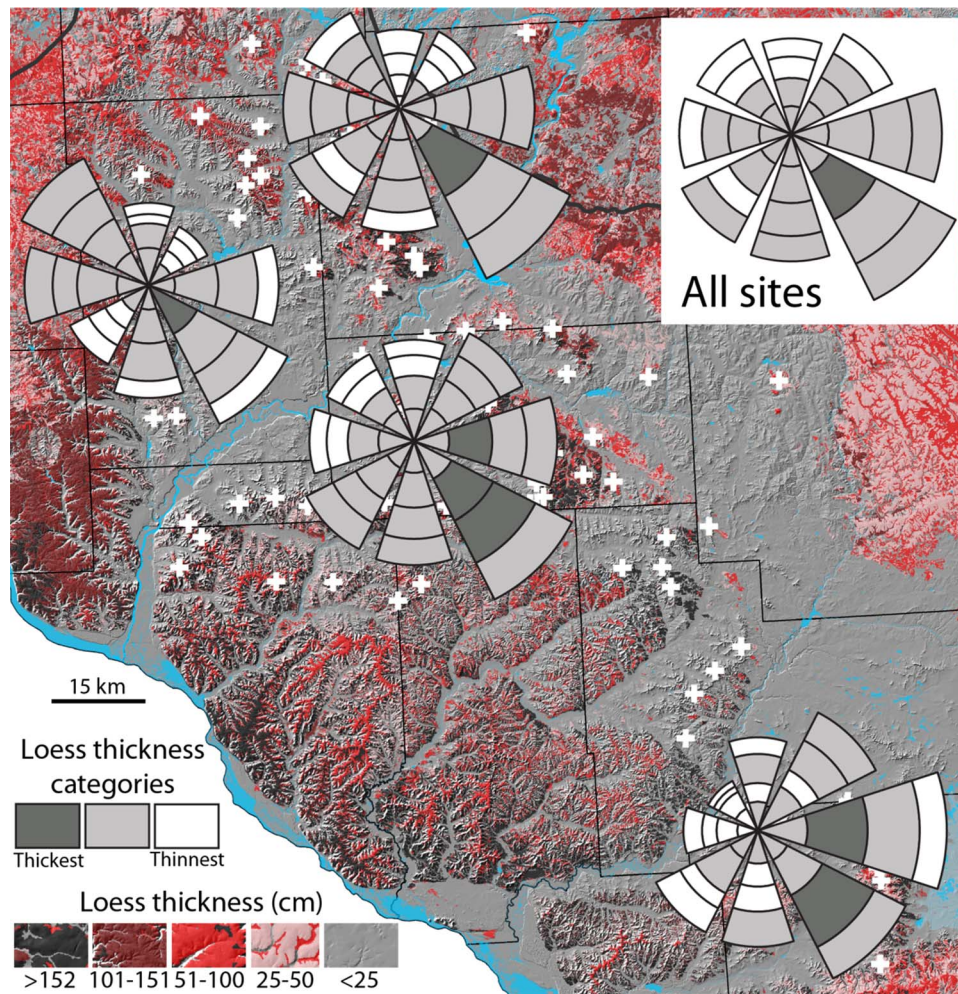
Figure 6. (color online) Loess patterns in the vicinity of bedrock uplands, shown as rose diagrams. Data are shown for all sites combined and for areal subsets. Thicknesses were determined for four distances along eight cardinal directions. Wedge lengths are proportional to the summed average loess thicknesses along the sample points, whereas the grayscale images of each wedge section reflect mean loess thicknesses at that distance from the ridgetop. Some sample sites are covered by the rose diagrams.

Pepin, and Eau Claire County soil surveys, are consistent with our sand sheet interpretation (Thomas, 1977; Jakel and Dahl, 1989; Meyer, 2002, 2004). Collectively, these series are widespread across the LCRV. The Dunn and Pepin County soil surveys (Meyer, 2002, 2004) explicitly state an eolian origin for sands in the following series: Boplain sand, Chelsea fine sand, Drammen loamy sand, Garne loamy sand, and Plainbo sand.

Low-order drainages exiting bedrock uplands are occasionally dammed by sand sheets, forming small lakes/wetlands (Figs. 8 and 9). Characteristic of these eolian-dammed drainages are closed depressions. These depressions, which we interpret to be deflation hollows, are primarily observed on the Wissota Terrace and older outwash surfaces.

Our current understanding of the depositional chronology of sand sheets, eolian-dammed drainages, and deflation hollows is based on spatial and stratigraphic relationships, as well as mapped units of soil series we interpret as having formed in eolian sands. Soils consistent with our sand sheet interpretation are reported in all county soil surveys in the

region. Most sand sheet deposits are underlain by sandstone residuum or by outwash deposits associated with pre-Wisconsin glaciations (River Falls Formation) or the Late Wisconsin glaciation (Copper Falls Formation) (Syverson, 2007). This relationship suggests these sands may have been active during the waning stages of the last glacial maximum. Sand sheet deposits underlain by terrace fill within the LCRV confirm that eolian sand mobilization here continued into the early Holocene (Faulkner et al., 2016).

Sand sheets, eolian-dammed drainages, and deflation hollows are often located in proximity to other more readily recognized eolian landforms (i.e., parabolic and linear dunes). The latter group of eolian features provides clear insight into paleowind direction, based on their distribution within the LCRV. They become progressively more common to the east and southeast across the region. More locally, eolian-dammed drainages and deflation hollows are commonly, but not exclusively, observed on west- and northwest-facing bedrock slopes that lie to the east and southeast of outwash plains (and locally, sandy till of the River Falls
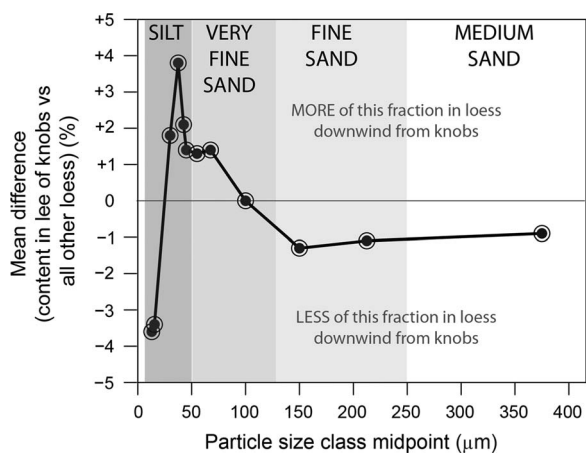
Figure 7. Mean differences in particle-size concentrations (expressed as percentage of the whole <2 mm "filtered" fraction) for loess at sites in the immediate lee (mainly southeast) of bedrock uplands versus loess at 2224 sites throughout Wisconsin and Michigan's Upper Peninsula. A value of zero implies that loess in the lee of bedrock uplands is no different, for that fraction, than loess generally across Wisconsin and northern Michigan.

Formation). Deflation hollows are often located immediately west of dunes that dam local drainages. Sand sheets also become progressively thicker (up to 1–2 m thick), as well as more widespread, to the east and southeast in the LCRV. Collectively, these features all suggest that eolian mobilization of sand in the region occurred in response to winds from the west and northwest.

Parabolic dunes

Parabolic dunes are crescent-shaped features that result from a predominant or unidirectional wind regime, with arms usually anchored by vegetation in the upwind direction (Lancaster, 2009). Parabolic dunes occur throughout the study area, ranging in height from <3 to 20 m (Fig. 8). They are predominantly found on the southern and eastern margins of the LCRV, although they do occur elsewhere, and in proximity to terrace scarps of the Chippewa River (Figs. 8 and 9). Some parabolic dunes are found within or to the southeast or east of sand sheets (Fig. 9). Others occur on outwash plains or sometimes in close proximity to linear dunes. Some irregularly shaped parabolic dunes have coalesced to form ridges, morphologically similar to transverse dune ridges.

We investigated a typical parabolic dune in Putnam Park, within the city of Eau Claire (Figs. 2 and 10; Larson et al., 2008). RSD is one of many parabolic dunes (up to 6 m high and 50 m in diameter) that occur immediately adjacent to the scarp of the Wissota Terrace. Initial research revealed that the RSD and those nearby are composed of well-sorted sands, with mean particle sizes in the lower-medium sand fraction (0.25–0.35 mm diameter), consistent with eolian sands. GPR surveys of the RSD also revealed internal structures consistent with migrating slip faces that would have formed on

northwesterly winds (Fig. 11). Larson et al. (2008) concluded that the RSD and similar landforms are cliff-top (or perched) dunes (Jennings, 1967; Saye et al., 2006), formed as northwest winds entrained sand exposed in terrace escarpments, as the Chippewa River was actively eroding laterally into Wissota Terrace fill (Fig. 10). Dune growth atop large, sandy escarpments is not uncommon in the region (e.g., Anderton and Loope, 1995; Arbogast, 2000).

Under the cliff-top dune model of Larson et al. (2008), the formation of the RSD should be directly linked to processes associated with Chippewa River incision. Based on the time-transgressive incision model of Faulkner et al. (2016), the Chippewa River did not incise below the Wissota Terrace near RSD until sometime after 8.9 ka. This 8.9 ka age is based on OSL ages from a vertical profile of terraces >15 km downstream of the RSD. If the cliff-top model is accurate, this chronology implies that the RSD and other dunes in this area are Holocene-aged landforms.

To test this hypothesis, luminescence dating was conducted on the RSD and in the Wissota Terrace alluvium underlying the RSD (Table 1). The dates from Wissota Terrace alluvium beneath the RSD (RSDshldr Wissota Terrace; Table 1) agree with the long period of glaciofluvial aggradation that largely filled the LCRV in the Late Pleistocene (Faulkner et al., 2016). Dates from sites farther downstream indicate that the Wissota Terrace surface remained the active floodplain several thousand years after these dates, later incising (>8.9 ka) and abandoning the Wissota Terrace tread in the vicinity of RSD in the mid-Holocene (Faulkner et al., 2016).

The age of the intermediate terraces (T-2 and T-3) located at the base of the Wissota Terrace escarpment (Fig. 10) are unknown at present. Faulkner et al. (2016) identified six terraces in the LCRV below the Wissota Terrace and informally named them T-1 (the lowest) through T-6. According to this naming scheme, the Wissota Terrace would be T-7. Based on the ages of correlated terrace surfaces downstream, the T-3 terrace surface was abandoned sometime after 4.7 ka. However, this does not preclude the area below and near the RSD from being an active channel prior to the formation of the local T-3 terrace surface. Currently, both the local T-2 and T-3 terraces occupy this landscape position, suggesting that this large meander scar may have existed as an active meander through vertical incision events, and older terraces may have been removed during formation of the T-3 meander. Indeed, locally four higher terraces (T-4, T-5, T-6, and Wissota) are in close proximity to this location, pointing to active incision of the Chippewa River near this site (Figs. 2 and 10) from after 8.9 ka through sometime after 4.7 ka, but before 2.3 ka (T-1 terrace). This incision would have exposed alluvium to wind, opening up a sediment source for the RSD and other cliff-top dunes.

The ages of the sands at the RSD crest, shoulder, and foot slope are substantially younger than the Wissota Terrace fill, as expected (Table 1). These dates are tightly clustered, even at depth, between 5.79 and 6.72 ka, suggesting that the RSD stabilized sometime in the mid-Holocene. Further dating of
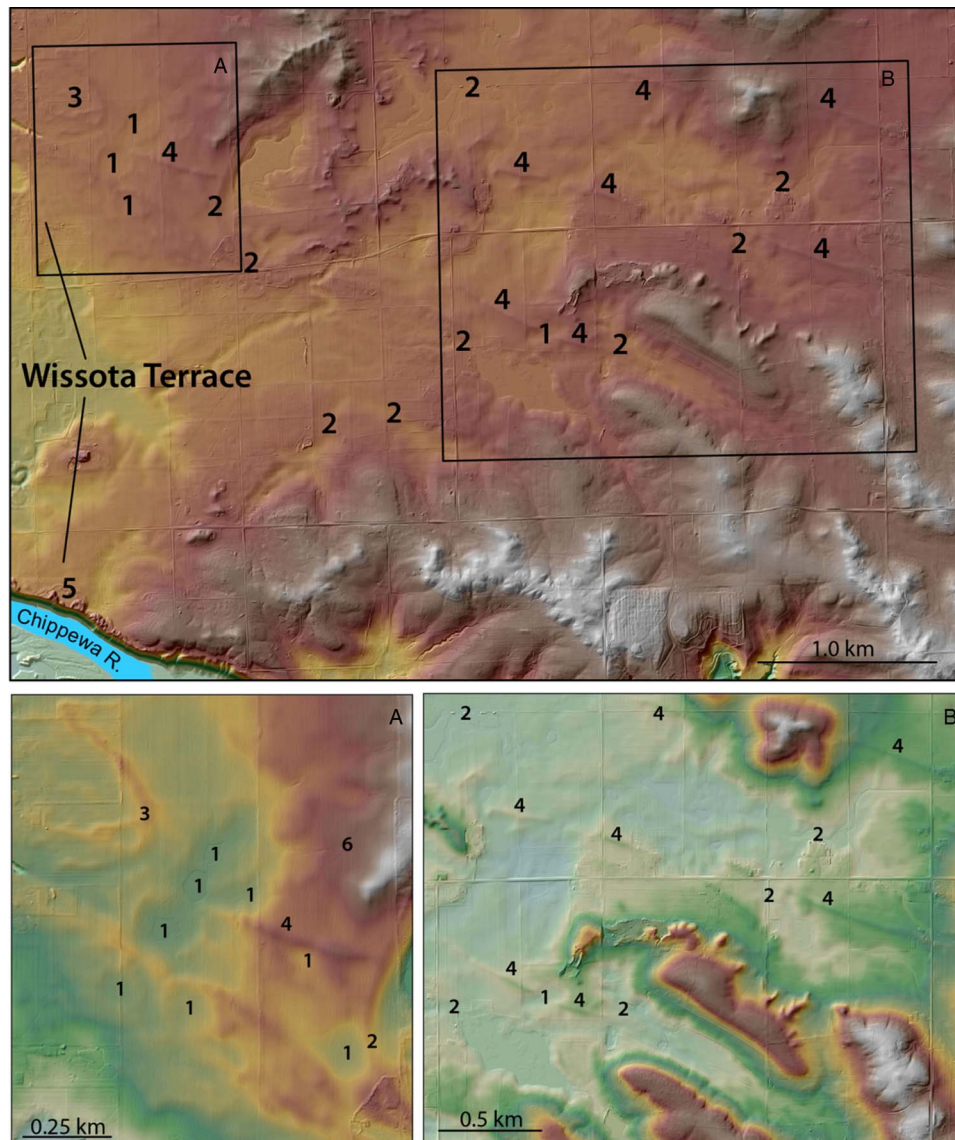
Figure 8. (color online) Broad overview maps of eolian features in western Eau Claire County: deflation hollows (1), eolian dammed drainages (2), a parabolic dune (3), linear dunes (4), parabolic dunes in cliff-top position adjacent to the Wissota Terrace scarp (5), and a possible sand ramp (6). Rectangles indicate the extents of panels A and B. Elevations on this map range from 229 m (Chippewa River) to 311 m.

the terraces in this area will help refine this chronology vis-à-vis its connection to the Faulkner et al. (2016) incision model, if the RSD and neighboring dunes are, indeed, cliff-top dunes (Larson et al., 2008). Alternatively, the RSD may have formed during the dry, warmer conditions of the mid-Holocene, not unlike those recorded regionally (Grigal et al., 1976; Keen and Shane, 1990; Dean et al., 1996).

Despite the uncertainty regarding the formation of the RSD, this mid-Holocene–aged parabolic dune can be used infer paleowind direction at the time of deposition (Lancaster, 2009). At the RSD site, GPR profiles show slip-face orientation indicative of northwest-to-southeast winds (Fig. 11). Parabolic dune orientations elsewhere in the LCRV (Figs. 8, 9, 12, and 13) also point to west-northwesterly and northwesterly winds. We did not use irregularly shaped parabolic dunes (or those that have coalesced into forms

morphologically similar to transverse dune ridges) to infer paleowind directionality. Nonetheless, the orientations of those landforms also appear consistent with west-northwesterly and northwesterly winds. The few parabolic dunes that show a southwest-to-northeast orientation are in cliff-top positions adjacent to the Wissota Terrace. Because these dunes are constrained in their formation by the cliff edge, they do not disprove the conclusions drawn previously, for parabolic dunes on the lowlands of the LCRV.

Linear dunes

Linear dunes are elongate, eolian depositional forms marked by their parallelism to the direction of net sediment transport (Fryberger and Dean, 1979; Lancaster, 1982, 2009;
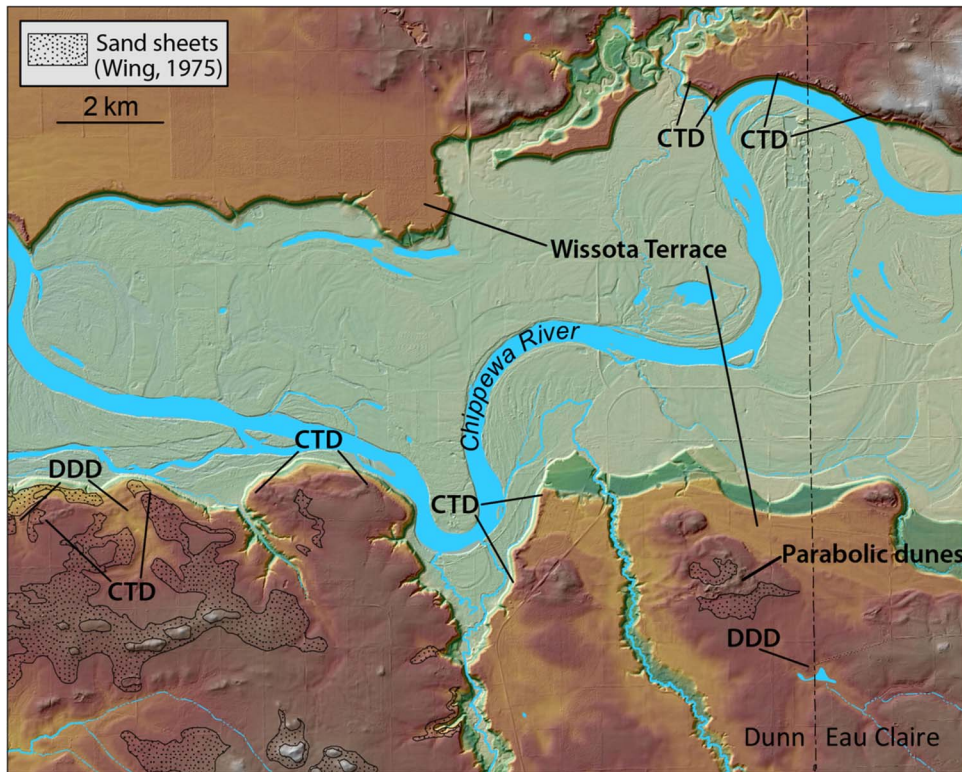
Figure 9. (color online) Sand sheets, parabolic dunes, cliff-top dunes (CTD), and dune-dammed drainages (DDD) present along the Chippewa River near the Dunn County–Eau Claire County border. Dunes are in cliff-top positions adjacent to terrace deposits and overlying pre–Late Wisconsinan glaciofluvial sediment. Note: Soil series descriptions consistent with our eolian sand sheet interpretation are more widespread than the areas identified as sand sheets in the Dunn County soil survey (Meyer, 2004). Similarly, soil series descriptions consistent with our sand sheet interpretation in the Eau Claire County soil survey (Thomas, 1977) are also widespread, but not explicitly identified as such. Elevations on this map range from 221 m (Chippewa River) to 306 m.

Tsoar, 1989; Livingstone and Warren, 1996; Rubin and Hesp, 2009). New LIDAR data for the LCRV brought to light a number of northwest-to-southeast trending linear features that were field checked and interpreted as dunes (Fig. 13). These linear dunes are subtle; most are 1.5–3.0 m high

and ≈100 m wide, and many exceed 1 km in length. They are roughly symmetrical in cross section, although some are distinctly asymmetrical, and have generally uniform relief. Their eastern ends often grade smoothly into the adjacent plain. Sometimes, however, they are associated with low,
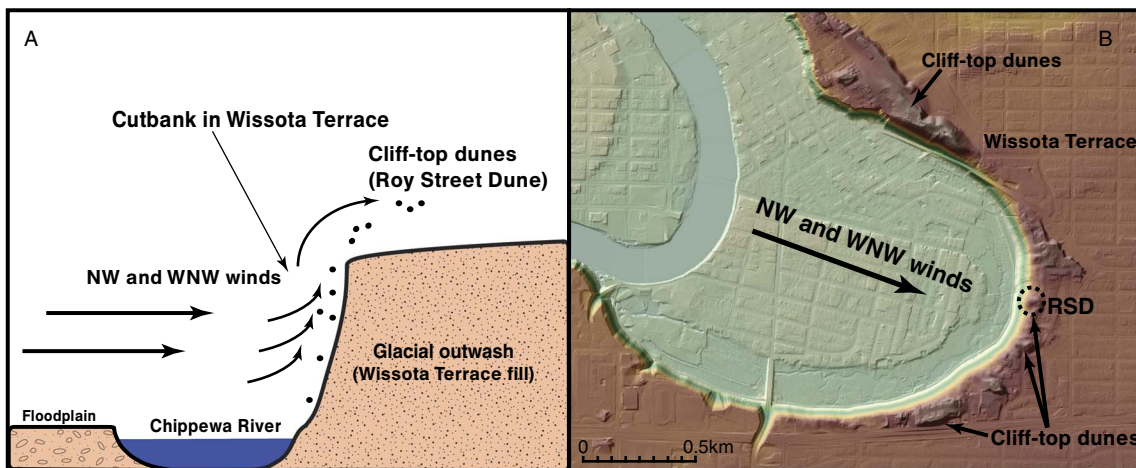

Figure 10. (color online) Cliff-top dunes in the city of Eau Claire. (A) Model of cliff-top dune formation for the Roy Street Dune (RSD), after Larson et al. (2008). Dune-forming winds were best able to entrain sand exposed in the alluvium when the Chippewa River was eroding laterally into terrace fill. (B) Map view of the area near the RSD. Elevations on this map range from 231 (Chippewa River) to 289 m. NW, northwest; WNW, west-northwest.
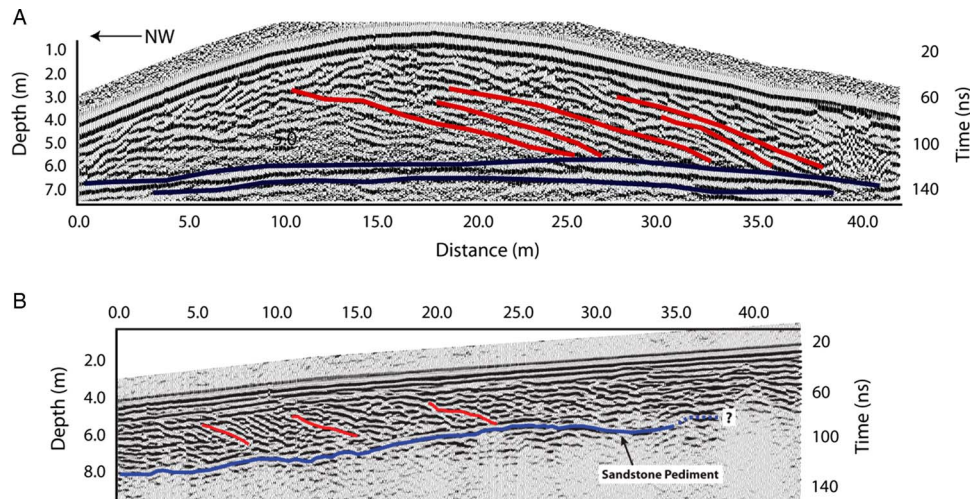
Figure 11. A 200 MHz ground-penetrating radar (GPR) transect of the Roy Street Dune (A), taken at 0.1 m/ns, and a 225 MHz GPR transect of the Northstar Sand Ramp (B), taken at 0.13 m/ns. Red lines highlight reflection patterns indicative of progressive slip-face migration. Blue lines highlight the contact between dune sediment and alluvium of the Wissota Terrace (Roy Street Dune) or dune sediment and the underlying bedrock (Northstar Sand Ramp). Different shades of blue indicate the strength of the GPR reflections. The lithologic contact below the Wissota Terrace in panel A has multiple horizontal reflections that are clear, so we punctuated that reflection with darker lines. Both GPR transects reveal that these eolian landforms were derived from westerly to west-northwesterly winds. After Larson et al. (2008). (For interpretation of the references to color in this figure legend, the reader is referred to the web version of this article.)

irregular dune forms. In either case, the western ends of the dunes are more sharply defined than the eastern ends. Although not specifically identified in NRCS county soil surveys, the dunes are associated with surface soils texturally consistent with eolian sands.

Our understanding of the age of these linear dunes is informed mainly by stratigraphic relationships. Most of these dunes are underlain by dissected outwash of the River Falls Formation or by Late Wisconsin outwash of the Copper Falls Formation (Syverson, 2007). We know of no such dunes that occur on the Holocene-aged Wissota Terrace, or on treads of younger LCRV terraces, suggesting a Late Pleistocene age.

The linear dunes in the study area all have a broadly northwest-to-southeast orientations (Figs. 12 and 13), suggesting formation by west-northwesterly and northwesterly winds. Well-defined western ends and tapering eastern margins that blend into the surrounding landscape also support this conclusion.
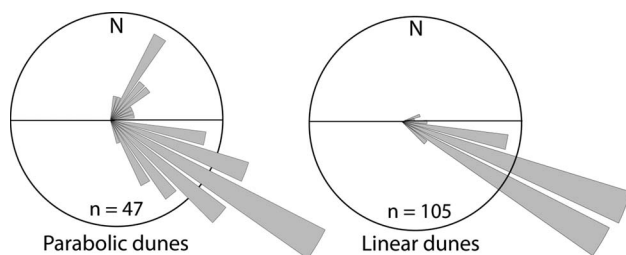

Figure 12. Rose diagrams showing the orientations of parabolic and linear dunes in the study area. Included in this data set are only those parabolic dunes that are sufficiently well preserved to confidently determine orientation.

Sand ramps

Few studies have examined sand ramps in environments outside of the contemporary arid zone; only a mention of sand ramps near the Root River, Minnesota, suggests that these forms may be widespread in the upper Midwest, USA (Hanson et al., 2015). We focused on the NSR (Fig. 5) as a representative form in the LCRV. Sediments at the NSR are dominated by well-sorted, fine to fine-medium loamy sands. Largely devoid of coarse fragments, parts of the sand ramp are nonetheless interbedded with gravelly colluvial debris derived from the bedrock beneath the sand ramp. Visual mineralogical investigations of sand grains in the NSR are consistent with Wissota Terrace fill mineralogy, rather than the uniformly quartz-rich sandstone mineralogy of the bedrock slope and ridge that the NSR overlies. We interpret this mineralogical distinction to indicate that the sands of the NSR accumulated contemporaneously with an active Wissota Terrace outwash surface (i.e., the latter was the source of sands in the NSR).

The three luminescence dates from the NSR, collected approximately halfway up the slope, range from 10.85 to 10.12 ka, indicating a short depositional interval (Table 1). These ages are significantly older than the incision of the Chippewa River that abandoned the Wissota Terrace. The difference in age between the NSR sands and the Chippewa River incision abandoning the Wissota outwash surface, along with the mixed mineralogy of the NSR sediments, points to the Wissota outwash surface as the likely sand source for the NSR.

The location of the NSR suggests transport of sands, up and onto the underlying bedrock slope (pediment), on
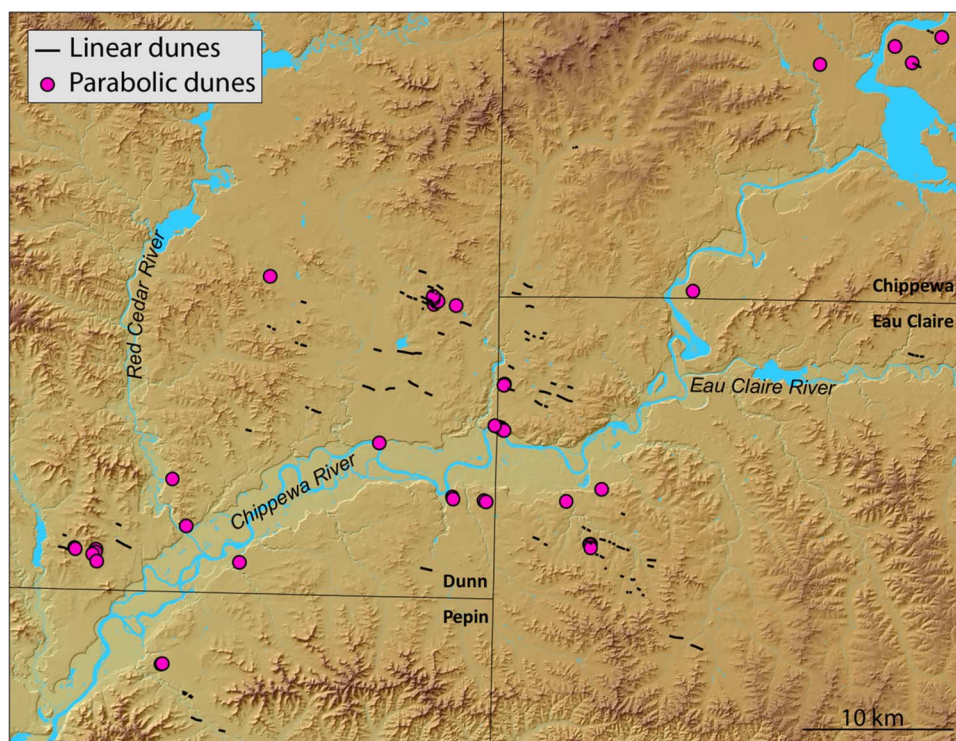
Figure 13. (color online) The lower Chippewa River valley and adjacent portions of western Wisconsin, showing the locations of major linear and parabolic dunes. The comparatively low resolution of Dunn County LIDAR (light detection and ranging) may explain an apparent lack of linear dunes in that portion of the figure. Only parabolic dunes sufficiently well preserved to determine orientation confidently are shown on this map. Reworked and eroded parabolic dunes and parabolic dunes that have coalesced into a morphology consistent with transverse dunes are not shown. Elevations on this map range from 211 m (Chippewa River) to 400 m.

westerly winds. Additional evidence for west-to-east transport comes from high-angle reflections, recorded in GPR imagery, which we interpret as eastward (and uphill) migrating eolian slip faces (Fig. 11). Finally, as is common at many bedrock uplands in the region, the sands on the western flank of the ridge that underlies the NSR yield to silt-rich loess on the eastern (lee) slope. Based on these data, and the presence of numerous ventifacted boulders on the surfaces of older glacial deposits in the Chippewa valley (Johnson, 1986; Syverson, 2007), we conclude that strong westerly winds concurrently formed the NSR on the west-facing slope and the loess deposits on the east-facing slope. Our field observations indicate that sand ramps like the NSR are ubiquitous in similar landscape positions across the LCRV, as are loess deposits on the lee sides of bedrock uplands (Fig. 3).

CONCLUSIONS

Some areas near the former ice margin in the northern Great Lakes region show on-ground evidence for easterly, or at least widely variable, winds during the Late Pleistocene deglacial period (Vader et al., 2012; Luehmann et al., 2013; Schaetzl and Attig, 2013; Schaetzl et al., 2016), providing on-the-ground support for the COHMAP model (COHMAP

Members, 1988). Despite being immediately south of the former ice front, eolian landforms and sediments in the LCRV show little evidence of having been formed by easterly winds. Instead, eolian landforms and sediments—including dune sand morphology and stratigraphy and loess thicknesses and textures—indicate that eolian systems here were controlled by west-northwesterly and northwesterly winds. These winds were strong enough to (1) form ventifacts; (2) transport sand up and onto the western margins of bedrock uplands, as sand ramps; and (3) transport sand up and onto the tops of cutbanks of the Chippewa River, as clifftop dunes. Particularly impressive is an array of linear and parabolic dunes on the sandy lowlands of the LCRV that also support formation on west-northwesterly and northwesterly winds.

Together, these data paint a picture of a sandy landscape, impacted by loess from western sources, during the Late Pleistocene and into the early Holocene, with a myriad of eolian features forming in the valley proper. The latter include features associated with processes of both eolian erosion and deposition, including subsequent remobilization. Spatially and temporally intermittent transport of eolian sands likely helped to remobilize some of the loess, such that most lowland areas are devoid of loess and are dominated by deflation hollows and various types of small dunes. Much of the remobilized loess was mixed into the underlying sediment or transported out of the region, while some was

deposited as thick loess in the lee of bedrock uplands. Further work will help constrain the timing of the eolian systems in the region and therefore better link this suite of eolian activity to the paleoclimatic record.

ACKNOWLEDGEMENTS

REFERENCES

Aitken, M.J., 1998. An Introduction to Optical Dating: The Dating of Quaternary Sediments by the Use of Photon-Stimulated Luminescence. Oxford University Press, New York.

Anderton, J.B., Loope, W.L., 1995. Buried soils in a perched dunefield as indicators of late Holocene lake-level change in the Lake Superior basin. *Quaternary Research* 44, 190–199.

Andrews, G.W., 1965. Late Quaternary geologic history of the lower Chippewa valley, Wisconsin. *Geological Society of America Bulletin* 76, 113–124.

Arbogast, A.F., 2000. Estimating the time since final stabilization of a perched dune field along Lake Superior. *Professional Geographer* 52, 594–606.

Arbogast, A.F., Luehmann, M.D., Miller, B.A., Wernette, P.A., Adams, K.M., Waha, J.D., O'Neil, G.A., Tang, Y., Boothroyd, J. J., Babcock, C.R., Hanson, P.R., Young, A.R., 2015. Late-Pleistocene paleowinds and aeolian sand mobilization in north-central Lower Michigan. *Aeolian Research* 16, 109–116.

Arbogast, A.F., Luehmann, M.D., Monaghan, W.G., Lovis, W.A., Wang, H., 2017. Paleoenvironmental and geomorphic significance of bluff-top dunes along the Au Sable River in Northeastern Lower Michigan, USA. *Geomorphology* 297, 112–121.

Attig, J.W., Bricknell, M., Carson, E.C., Clayton, L., Johnson, M. D., Mickelson, D.M., Syverson, K.M., 2011a. Glaciation of Wisconsin. 4th ed. Educational Series Publication, 36. Wisconsin Geological and Natural History Survey, Madison, WI.

Attig, J.W., Clayton, L., Mickelson, D.M., 1985. Correlation of late Wisconsin glacial phases on the western Great Lakes. *Geological Society of America Bulletin* 96, 1585–1593.

Attig, J.W., Hanson, P.R., Rawling, J.E. III, Young, A.R., Carson, E.C., 2011b. Optical ages indicate the southwestern margin of the Green Bay Lobe in Wisconsin, USA, was at its maximum extent until about 18,500 years ago. *Geomorphology* 130, 384–390.

Baker, G.S., Jol, H.M., 2007. Stratigraphic Analyses Using GPR. Special Paper 432. Geological Society of America, Boulder, CO.

Baker, R.W., Diehl, J.F., Simpson, T.W., Zelazney, L.W., Beske-Diehl, S., 1983. Pre-Wisconsin glacial stratigraphy, chronology and paleomagnetics of west-central Wisconsin. *Geological Society of America Bulletin* 94, 1442–1449.

Bettis, E.A. III, Muhs, D.R., Roberts, H.M., Wintle, A.G., 2003. Last glacial loess in the conterminous USA. *Quaternary Science Reviews* 22, 1907–1946.

Bristow, C.S., 2009. Ground penetrating radar in aeolian dune sands. In: Jol, H.M. (Ed.), Ground Penetrating Radar: Theory and Applications. Elsevier, Amsterdam, pp. 273–297.

Brown, B.A., 1988. Bedrock Geology of Wisconsin, West-Central Sheet. Wisconsin Geological and Natural History Survey Map Series 88-7. Wisconsin Geological and Natural History Survey, University of Wisconsin Extension, Madison.

Bryson, R.A., Wendland, W.M., 1967. Radiocarbon Isochrones of the Retreat of the Laurentide Ice Sheet. Technical Report 35. Department of Meteorology, University of Wisconsin, Madison.

Campbell, M.C., Fisher, T.G., Goble, R.J., 2011. Terrestrial sensitivity to abrupt cooling recorded by aeolian activity in northwest Ohio, USA. *Quaternary Research* 75, 411–416.

Carson, E.C., Hanson, P.R., Attig, J.W., Young, A.R., 2012. Numeric control on the late-glacial chronology of the southern Laurentide Ice Sheet derived from ice-proximal lacustrine deposits. *Quaternary Research* 78, 583–589.

Clayton, L., Attig, J.W., Mickelson, D.M., 2001. Effects of late Pleistocene permafrost on the landscape of Wisconsin, USA. *Boreas* 30, 173–188.

COHMAP Members, 1988. Climatic changes of the last 18,000 years: observations and model simulations. *Science* 241, 1043–1052.

Colgan, P.M., Amidon, W.H., Thurkettle, S.A., 2017. Inland dunes on the abandoned bed of Glacial Lake Chicago indicate eolian activity during the Pleistocene-Holocene transition, southwestern Michigan, USA. *Quaternary Research* 87, 66–81.

David, P.P., 1981. Stabilized dune ridges in northern Saskatchewan. *Canadian Journal of Earth Sciences* 18, 286–310.

Dean, W.E., Ahlbrandt, T.S., Anderson, R.Y., Bradbury, J.P., 1996. Regional aridity in North America during the middle Holocene. *Holocene* 6, 145–155.

Faulkner, D., Larson, P.H., Jol, H.M., Running, G.L., Loope, H.M., Goble, R.J., 2016. Episodic incision and terrace formation resulting from abrupt late-glacial base-level fall, lower Chippewa River, Wisconsin, USA. *Geomorphology* 266, 75–95.

Fryberger, S., Dean, G., 1979. Dune forms and wind regime. In: McKee, E.D. (Ed), Introduction to a Study of Global Sand Seas (U.S. Geological Survey Professional Paper 1052. 137–170.

Galbraith, R.F., Roberts, R.G., 2012. Statistical aspects of equivalent dose and error calculation and display in OSL dating: an overview and some recommendations. *Quaternary Geochronology* 11, 1–27.

Grigal, D.F., Severson, R.C., Goltz, G.E., 1976. Evidence of eolian activity in north-central Minnesota 8,000 to 5,000 yr ago. *Geological Society of America Bulletin* 87, 1251–1254.

Guerin, G., Mercier, N., Adamiec, G., 2011. Dose-rate conversion factors: update. *Ancient TL* 29, 5–8.

Ham, N.R., Attig, J.W., 1997. Pleistocene Geology of Lincoln County, Wisconsin. Bulletin 93. Wisconsin Geological and Natural History Survey, University of Wisconsin Extension, Madison.

Hanson, P.R., Mason, J.A., Jacobs, P.M., Young, A.R., 2015. Evidence for bioturbation of luminescence signals in eolian sand on upland ridgetops, southeastern Minnesota, USA. *Quaternary International* 362, 108–115.

Havholm, K.G., Bergstrom, N.D., Jol, H.M., Running, G.L., 2003. GPR survey of a Holocene aeolian/fluvial/lacustrine succession, Lauder Sandhills, Manitoba, Canada. In Bristow, C.S., Jol, H.M.

(Eds.), Ground Penetrating Radar in Sediments. *Geological Society, London, Special Publications* 211, 47–54.

Hesp, P.A., 1981. The formation of shadow dunes. *Journal of Sedimentological Research* 51, 101–111.

Hesp, P.A., Smyth, T.A.G., 2017. Nebkha flow dynamics and shadow dune formation. *Geomorphology* 282, 27–38.

Hobbs, W.H., 1943. The glacial anticyclone and the continental glaciers of North America. *Proceedings of the American Philosophical Society* 86, 368–402.

Hole, F.D., 1976. Soils of Wisconsin. University of Wisconsin Press, Madison.

Jakel, D.E., Dahl, R.A., 1989. Soil Survey of Chippewa County, Wisconsin. Soil Conservation Service, U.S. Government Printing Office, Washington, DC.

Jennings, J.N., 1967. Cliff-top dunes. *Geographical Research* 5, 40–49.

Johnson, M.D., 1986. Pleistocene Geology of Barron County, Wisconsin. Information Circular 55. Wisconsin Geological and Natural History Survey, Madison, WI.

Jol, H.M., 2009. Ground Penetrating Radar: Theory and Applications. Elsevier, Amsterdam.

Jol, H.M., Bristow, C.S., 2003. GPR in sediments: advice on data collection, basic processing and interpretation, a good practice guide. In: Bristow, C.S., Jol, H.M. (Eds.), Ground Penetrating Radar in Sediments. *Geological Society, London, Special Publications* 211, 9–27.

Jol, H.M., Bristow, C.S., Smith, D.G., Junck, M.B., Putnam, P., 2003. Stratigraphic imaging of the Navajo Sandstone using ground-penetrating radar. *Leading Edge* 22, 882–887.

Kasse, C., 1997. Cold-climate aeolian sand-sheet formation in north-western Europe (c. 14–12.4 ka): a response to permafrost degradation and increased aridity. *Permafrost and Periglacial Processes* 8, 295–311.

Keen, K.L., Shane, L.C.K., 1990. A continuous record of Holocene eolian activity and vegetation change at Lake Ann, east-central Minnesota. *Geological Society of America Bulletin* 102, 1646–1657.

Kilibarda, Z., Blockland, J., 2011. Morphology and origin of the Fair Oaks Dunes in NW Indiana, USA. *Geomorphology* 125, 305–318.

Knox, J.C., Bartlein, P.J., Webb, T. III, Clayton, L., Frolking, T.A., Hole, F.D., Attig, J.W., *et al*. 1982. *Quaternary History of the Driftless Area with Special Papers*. Wisconsin Geological and Natural History Survey, Madison, WI.

Koster, E.A., 1988. Ancient and modern cold-climate aeolian sand deposition: a review. *Journal of Quaternary Science* 3, 69–83.

Krist, F., Schaetzl, R.J., 2001. Paleowind (11,000 BP) directions derived from lake spits in northern Michigan. *Geomorphology* 38, 1–18.

Lancaster, N., 1982. Linear dunes. *Progress in Physical Geography* 6, 475–504.

Lancaster, N., 2009. Dune morphology and dynamics. In: Parsons, A., Abrahams, A.D. (Eds.), *Geomorphology of Desert Environments*. Springer, New York, pp. 557–595.

Larson, P.H., Dryer, W.P., Mc Donald, J., Baker, A., Running, G.L., Faulkner, D.J., Jol, H.M., 2008. Geomorphology of cliff-top parabolic dunes within the Lower Chippewa River Valley, Upper Putnam Park, Eau Claire, Wisconsin. Abstracts with Programs, Association of American Geographers Annual Meeting, Boston, MA.

Leigh, D.S., Knox, J.C., 1993. AMS radiocarbon age of the Upper Mississippi Valley Roxana Silt. *Quaternary Research* 39, 282–289.

Livingstone, I., Warren, A., 1996. Aeolian Geomorphology: An Introduction. Longman, Singapore.

Loope, W.L., Fisher, T.G., Jol, H.M., Goble, R.J., Anderton, J.B., Blewett, W.L., 2004. A Holocene history of dune-mediated landscape change along the southeastern shore of Lake Superior. *Geomorphology* 61, 303–322.

Luehmann, M.D., Schaetzl, R.J., Miller, B.A., Bigsby, M., 2013. Thin, pedoturbated and locally sourced loess in the western Upper Peninsula of Michigan. Aeolian. *Research* 8, 85–100.

Mason, J.A., 2015. Up in the refrigerator: geomorphic response to periglacial environments in the Upper Mississippi River basin, USA. *Geomorphology* 248, 363–381.

Mason, J.A., Nater, E.A., Zanner, C.W., Bell, J.C., 1999. A new model of topographic effects on the distribution of loess. *Geomorphology* 28, 223–236.

McSweeney, K., Leigh, D.S., Knox, J.C., Darmody, R.H., 1988. Micromorphological analysis of mixed zones associated with loess deposits of the midcontinental United States. In: Eden, D.N., Furkert, R.J. (Eds.), Loess: Its Distribution, Geology and Soils. Proceedings of the International Symposium on Loess, New Zealand. A.A. Balkema, Rotterdam, the Netherlands, pp. 117–130.

Meyer, T.A., 2002. Soil Survey of Pepin County, Wisconsin. Subset of MLRA 105. Natural Resources Conservation Service, U.S. Government Printing Office, Washington, DC.

Meyer, T.A., 2004. Soil Survey of Dunn County, Wisconsin. Subset of MLRA 105. Natural Resources Conservation Service, U.S. Government Printing Office, Washington, DC.

Mickelson, D.M., Clayton, L., Fullerton, D.S., Borns, H.W., 1983. The Late Wisconsin glacial record of the Laurentide Ice Sheet in the United States. In: Wright, H.E., Jr. (Ed.), Late Quaternary Environments of the United States Vol. 1, The Late Pleistocene. University of Minnesota Press, Minneapolis pp. 3–37.

Miller, B.A., Schaetzl, R.J., 2012. Precision of soil particle size analysis using laser diffractometry. *Soil Science Society of America Journal* 76, 1719–1727.

Murray, A.S., Wintle, A.G., 2000. Luminescence dating of quartz using an improved single aliquot regenerative-dose protocol. *Radiation Measurements* 32, 57–73.

Murray, A.S., Wintle, A.G., 2003. The single aliquot regenerative dose protocol: potential for improvements in reliability. *Radiation Measurements* 37, 377–381.

Olson, L.M., Larson, P.H., Hupy, J., Jol, H.M., Faulkner, D.J., Running, G.L., 2008. Late Quaternary eolian dunes and fluvial terraces of the lower Chippewa River valley. Abstracts with Programs, Association of American Geographers Annual Meeting, Boston, MA.

Ostrom, M.E., 1970. Lithologic Cycles in Lower Paleozoic Rocks of Western Wisconsin. Field Trip Guidebook for Cambrian-Ordovician Geology of Western Wisconsin. Information Circular No. 11. Wisconsin Geological and Natural History Survey, Madison, WI.

Prescott, J.R., Hutton, J.T., 1994. Cosmic ray contributions to dose rates for luminescence and ESR dating. *Radiation Measurements* 23, 497–500.

Rawling, J.E. III, Hanson, P.R., Young, A.R., Attig, J.W., 2008. Late Pleistocene dune construction in the central sand plain of Wisconsin, USA. *Geomorphology* 100, 494–505.

Rittenour, T.M., Blum, M.D., Goble, R.J., 2007. Fluvial evolution of the lower Mississippi River valley during the last 100-kyr glacial cycle: Response to glaciation and sea-level change. *Geological Society of America Bulletin* 119, 586–608.

Ritter, D.F., Kochel, R.C., Miller, J.R., 2002. Process Geomorphology. Waveland Press, Long Grove, IL.

Rubin, D.M., Hesp, P.A., 2009. Multiple origins of linear dunes on Earth and Titan. *Nature Geoscience* 2, 653–658.

Saye, S.E., Pye, K., Clemmensen, L.B., 2006. Development of a cliff-top dune indicated by particle size and geochemical characteristics: Rubjerg Knude, Denmark. *Sedimentology* 53, 1–21.

Schaetzl, R.J., 2012. Comment on: Mississippi Valley regional source of loess on the southern Green Bay Lobe land surface, Wisconsin (Quaternary Research 75:574-583, 2011). *Quaternary Research* 78, 149–151.

Schaetzl, R.J., Attig, J.W., 2013. The loess cover of northeastern Wisconsin. *Quaternary Research* 79, 199–214.

Schaetzl, R.J., Forman, S.L., Attig, J.W., 2014. Optical ages on loess derived from outwash surfaces constrain the advance of the Laurentide Ice Sheet out of the Lake Superior basin, USA. *Quaternary Research* 81, 318–329.

Schaetzl, R.J., Krist, F.J. Jr., Luehmann, M.D., Lewis, C.F.M., Michalek, M.J., 2016. Spits formed in Glacial Lake Algonquin indicate strong easterly winds over the Laurentide Great Lakes during Late Pleistocene. *Journal of Paleolimnology* 55, 49–65.

Schaetzl, R.J., Loope, W.L., 2008. Evidence for an eolian origin for the silt enriched soil mantles on the glaciated uplands of eastern Upper Michigan, USA. *Geomorphology* 100, 285–295.

Schaetzl, R.J., Luehmann, M.D., 2013. Coarse-textured basal zones in thin loess deposits: Products of sediment mixing and/or paleoenvironmental change? *Geoderma* 192, 277–285.

Scull, P., Schaetzl, R.J., 2011. Using PCA to characterize and differentiate the character of loess deposits in Wisconsin and Upper Michigan, USA. *Geomorphology* 127, 143–155.

Stanley, K.E., Schaetzl, R.J., 2011. Characteristics and paleoenvironmental significance of a thin, dual-sourced loess sheet, north-central Wisconsin. *Aeolian Research* 2, 241–251.

Syverson, K.M., 2007. Pleistocene Geology of Chippewa County, Wisconsin. Bulletin 103. Wisconsin Geological and Natural History Survey, Madison, WI.

Syverson, K.M., Colgan, P.M., 2004. The Quaternary of Wisconsin: a review of stratigraphy and glaciation history. In: Ehlers, J., Gibbard, P.L. (Eds.), Quaternary Glaciations: Extent and Chronology. Elsevier, Amsterdam, pp. 295–311.

Thomas, D.D., 1977. Soil Survey of Eau Claire County, Wisconsin. Soil Conservation Service, U.S. Government Printing Office, Washington, DC.

Tsoar, H., 1989. Linear dunes – forms and formation. *Progress in Physical Geography* 13, 507–528.

Vader, M.J., Zeman, B.K., Schaetzl, R.J., Anderson, K.L., Walquist, R.W., Freiberger, K.M., Emmendorfer, J.A., Wang, H., 2012. Proxy evidence for easterly winds in Glacial Lake Algonquin, from the Black River Delta in northern Lower Michigan. *Physical Geography* 33, 252–268.

Weidman, S., 1911. Reconnaissance Soil Survey of Part of North Western Wisconsin. Bulletin 23. Wisconsin Geological and Natural History Survey, Madison, WI.

Wing, G.N., Murray, A.S., 1975. Soil Survey of Dunn County, Wisconsin. Soil Conservation Service, U.S. Govt. Printing Office, Washington, DC.

Wintle, A.G., Murray, A.S., 2006. A review of quartz optically stimulated luminescence characteristics and their relevance in single-aliquot regenerative protocols. *Radiation Measurements* 41, 369–391.